**Contract No:**

This document was prepared in conjunction with work accomplished under Contract No. DE-AC09-08SR22470 with the U.S. Department of Energy.

**Disclaimer:**

# The Impact of Partial Crystallization on the Permeation Properties Bulk Amorphous Glass Hydrogen Separation Membranes

Kyle S. Brinkman[1] Elise B. Fox[1], Paul Korinko[1], Thad Adams[1] and Art Jurgensen[2]
[1]Materials Science and Technology Directorate, Savannah River National Laboratory (SRNL)
Aiken, SC 29808, U.S.A.
[2]Analytical Development, Savannah River National Laboratory (SRNL)
Aiken, SC 29808, U.S.A.

## ABSTRACT

It is recognized that hydrogen separation membranes are a key component of the emerging hydrogen economy. A potentially exciting material for membrane separations are bulk metallic glass materials due to their low cost, high elastic toughness and resistance to hydrogen "embrittlement" as compared to crystalline Pd-based membrane systems. However, at elevated temperatures and extended operation times structural changes including partial crystallinity may appear in these amorphous metallic systems. A systematic evaluation of the impact of partial crystallinity/devitrification on the diffusion and solubility behavior in multi-component Metallic Glass materials would provide great insight into the potential of these materials for hydrogen applications. This study will report on the development of time and temperature crystallization mapping and their use for interpretation of "in-situ" hydrogen permeation at elevated temperatures.

## INTRODUCTION

The development of metallic glasses in bulk form had led to a resurgence of interest into the utilization of these materials for a variety of applications. A potentially exciting application for these bulk metallic glass (BMG) materials is their use as composite membranes to replace high cost Pd/Pd-alloy membranes for enhanced gas separation processes. One of the major drawbacks to the industrial use of Pd-Pd/alloy membranes is that during cycling above and below a critical temperature an irreversible change takes place in the palladium lattice structure which can result in significant damage to the membrane. Furthermore, the cost associated with Pd-based membranes is a potential detractor for their continued use and bulk metallic glass alloys offer a potentially attractive alternative. Several BMG alloys have been shown to possess high permeation rates comparable to those measured for pure Pd metal[1, 2]. Both of these properties- high permeation and high strength/toughness potentially make these materials attractive for gas separation membranes that could resist hydrogen "embrittlement". However, a fundamental understanding of the relationship between partially crystalline "structure"/devitrification and permeation/embrittlement in these BMG materials is required in order to determine the operating window for separation membranes and provide additional input to material synthesis community for improved alloy design. This project aims to fill the knowledge gap regarding the impact of crystallization on the permeation properties of metallic glass materials.

## EXPERIMENT

Metallic glass samples with a nominal thickness of 25 microns in 2 inch wide ribbons were purchased from commercial sources (MetGlas Inc., Conway SC) with the compositions given in Table 1. Metglass ribbon samples were heated under vacuum to elevated temperatures for various times and quenched under argon to achieve different degrees of partial crystallinity. Samples were initially characterized from 10 to 90 degrees two theta on a PanAnalytical X-ray diffractometer in order to confirm the absence of detectable crystallization in the as-received baseline samples. Samples which were intentionally crystallized were characterized by XRD to determine the degree of crystallinity. An 651 model TA Instruments DSC was used to evaluate crystallization temperatures at scan rates of $10^{o}$C/min from $25^{o}$C up to $590^{o}$C in argon and 4% hydrogen 96% argon gas flowing at 30sccm. The instrument was temperature calibrated using an indium metal standard and the nominal metallic glass sample mass was ~8mg. Permeation test samples were sealed by crimping between two VCR fittings with a Ag plated Cu gasket which were then connected to a standard 2.12" CF flanges and helium leak tested to confirm lower than $1X10^{-7}$ std cc/second at 1 atmosphere pressure. Measurement of the steady state permeation flux was conducted under sub-atmospheric pressures (400 to 700 Torr), values typically used at the Savannah River Site for hydrogen isotope purification. The measured permeability was $5.3 \times 10^{-9}$ mol $H_2$ $m^{-1}$ $s^{-1}$ $Pa^{-1/2}$ for the 2826 alloy at $400^{o}$C and 700 torr pressure differential compared to Pd flux of $2 \times 10^{-8}$ mol $H_2$ $m^{-1}$ $s^{-1}$ $Pa^{-1/2}$[3-5].

**Table 1. Alloy composition investigated, purchased from Metglas company Inc. and Howmet Research Corporation[6].**

| Alloy | $T_1$cryst $^{o}$C | Fe | B | Cr | Mo | Co | Ni | Si |
|---|---|---|---|---|---|---|---|---|
| **2605S3A** | 521 | 85-95% | 1-5% | 1-5% | 0% | 0% | 0% | 1-5% |
| **2714A** | 551 | 7-13% | 1-5% | 0% | 0% | 75-90% | 1-5% | 7-13% |
| **2826** | 421 | 40-50 | 1-5% | 0% | 5-10% | 0.3% | 40-50% | 0% |
| **2605SA1** | 504 | 85-95% | 1-5% | 0% | 0% | 0.2% | 0.2% | 5-10% |
| Zr Alloy | **471** | ***Proprietary*** | | | | | | |

## RESULTS AND DISCUSSION

Firstly, calorimetric techniques were used to determine the temperature of crystallization and the energy released of the five commercial available Metglas alloys indicated in Table 1 and Figure 1 using a ramp rate of $10^{o}$C/min under a flowing argon atmosphere.

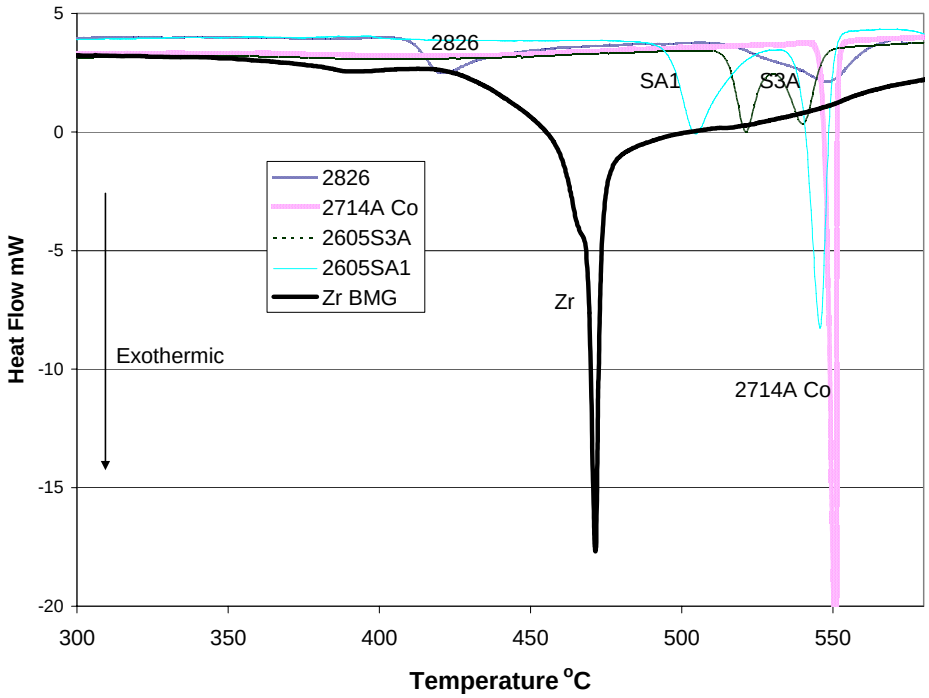


**Figure 1. Differential scanning calorimetry (DSC) performed on metglass alloys at 10°C/min under flowing Argon atmosphere 30sccm from 25°C to 590°C.**

The crystallization kinetics of a material may be determined from the peak temperature shift of the crystallization exotherm taken at different heating rates. Figure 2. shows the raw data from DSC scans taken of the 2826 alloy under argon atmosphere at 5, 10 and 20°C/min.

The shift of the crystallization peak may be used with equation 1 to obtain an activation energy and pre-exponential factor described as:

$$\ln\left(\frac{C}{Tp^2}\right) = -\frac{E}{k_b Tp} + A \qquad (1)$$

where C=heating rate °C/minute, Tp= peak crystallization temperature, E=activation energy (J/mol), $k_b$=boltzman constant and A=pre-exponential factor [7, 8]. From equation 1, a plot of $\ln(C/Tp^2)$ versut 1/Tp gives a slope equal to –E/k and the pre-exponential factor A. A plot of the data for the 2826 alloy is shown in figure 2b to determine the activation energy of 355 kJ/mol and a pre-exponential factor of $1.9X10^{22}$. The value of activation energy determined from DSC measurements agrees well with literature values of the activation energy (350kJ/mol) determined from microscopy studies used to determine the nucleation and growth rate as a function of temperature in 2826 metglass alloys[9]. Using the parameters from equation 1 and assuming an Arrehenius reaction rate is appropriate for the description of the rate constant as a function of temperature equation 2 is obtained.

$$k = A\exp\left(\frac{-E}{RT}\right) \qquad (2)$$

where k is the rate constant ($min^{-1}$), T is the specimen temperature, E and A are the same as described in equation 1. Previous studies have shown that metallic glass specimens can be well described by Johnson-Mehl-Avrami kinetic expressions such as:

$$X(t)=1-\exp(-kt^n) \quad (3)$$

Where x(t) is the fraction transformed at time t, n is an exponent experimentally determined, which reflects the nucleation rate taken to be 3.5 in this case from literature [10], k is the rate constant determined at temperature T from equation 2.

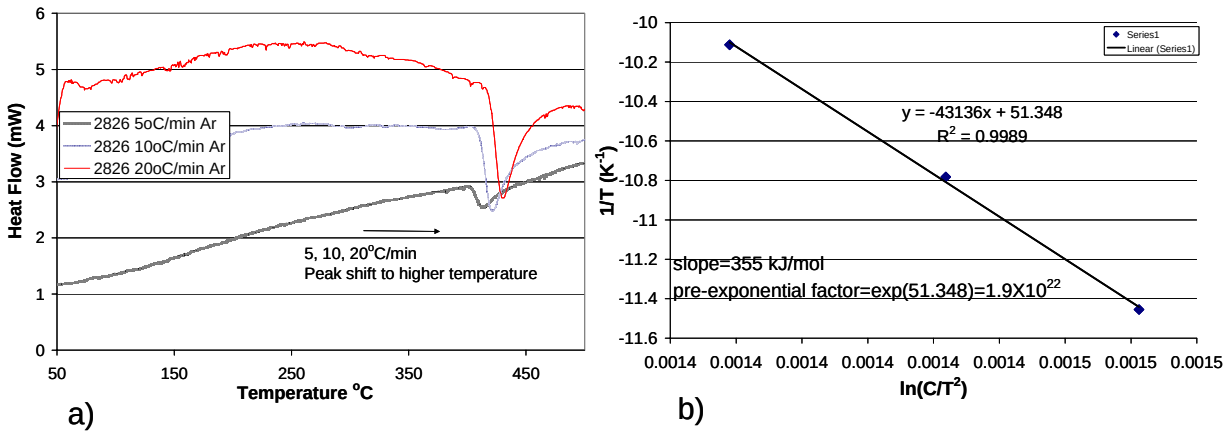


**Figure 2. a)DSC of 2826 metglass alloy in argon at 5, 10 and 20°C/minute heating rate showing an upward shift in peak crystallization temperataure wth increasing heating rate. b) Activation energy determination for 2826 alloy crystallization: plot of 1/T versus ln(C/T$^2$).**

Using equation 2 and 3, the crystallization fraction of the material can be determined as a function of time at various temperatures. A plot of this behavior for the 2826 metglass alloy is shown in Figure 2 for temperatures of 380, 400 and 420°C. Included in the plot is the experimental data for isothermal crystallization behavior of the 2826 alloy determined by DSC. The material was heated at 10°C/min up to 380°C and slowly ramped to 400°C at 2°C/min and held for 3 hours. The heat flow was corrected for thermal lag [8] by using an aluminum sample with the same mass as the 2826 metglass alloy. The area under the crystallization peak at time t was divided by the total area under the crystallization peak in order to determine x(t). The preceding kinetic analysis thus results in a temperature and time map of partial crystallinity in metglass materials which can be used to help interpret changes in elevated temperature permeation experiments.

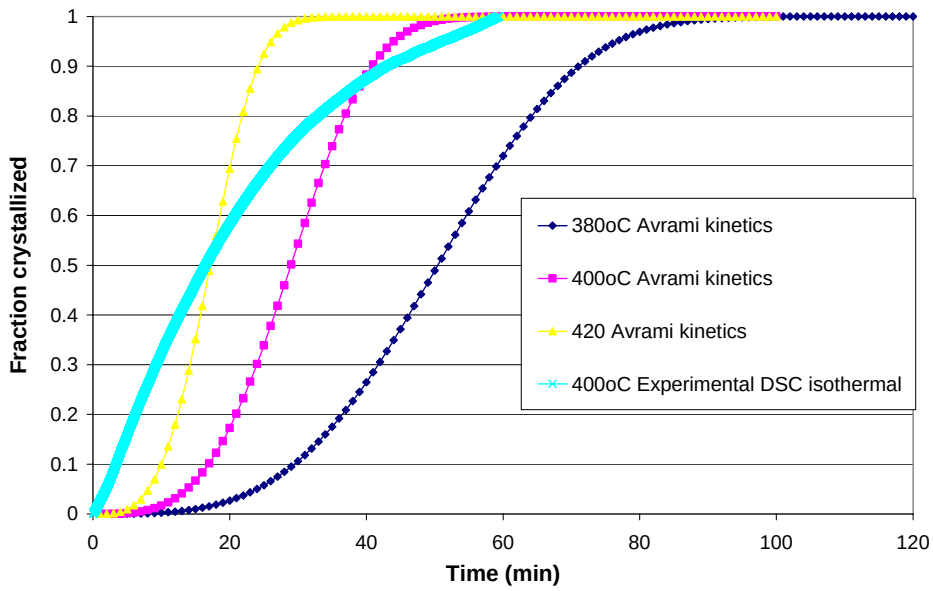


**Figure 3. Fraction crystallized from experimentally determined parameters and equations 2 and 3. Isothermal DSC crystallization data at 400°C included for comparison.**

The X-ray diffraction determined crystallinity of these samples is shown in figure 4 as compared to the as-received amorphous material indicating an increase in crystalline fraction identified as $Fe_{0.5}Ni_{0.5}$ with increasing time at 400°C in the 2826 alloy.

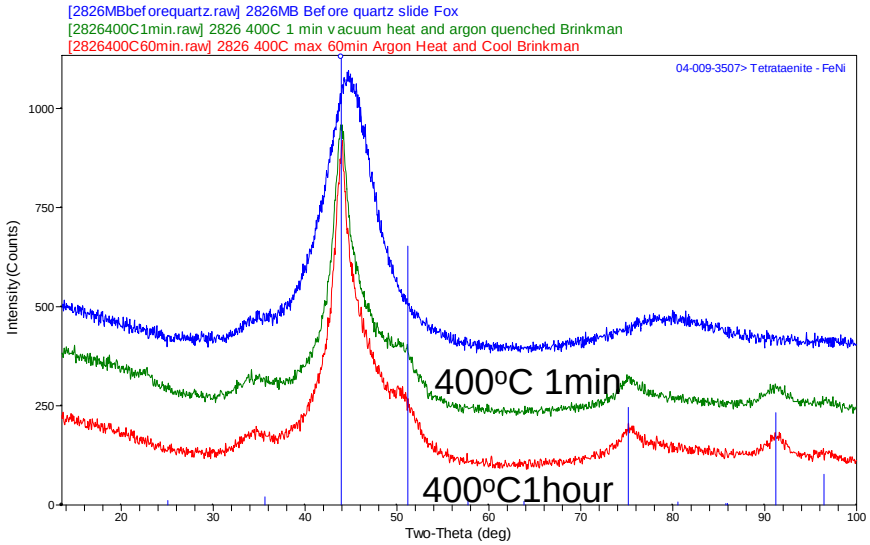


**Figure 4. XRD pattern of amorphous 2826 alloy and sample annealed to 400°C for 1 minute and 1 hour in vacuum, followed by argon quenching. Crystalline phase was identified as $Fe_{0.5}Ni_{0.5}$ FCC alloy ordered tetragonal superlattice with a=2.53 A, c=3.58 A.**

"In-situ" crystallization/permeation measurements are displayed in Figure 5 which depicts the measured total pressure and hydrogen partial pressure versus time and temperature for the

2826 metglass alloy. In the dynamic measurement displayed in figure 5, the permeation flux is directly proportional to the measured hydrogen partial pressure. Changes in the slope of this curve, dP/dt indicates apparent changes in the hydrogen flux. The hydrogen permeation is seen to increase with increasing temperature as expected. The time dependence of the flux at temperature shows an approximately steady decrease. At a temperature of 380$^{o}$C, the flux decreases over a four hour duration. From kinetic predictions shown in Figure 3 the material should be completely crystalline at this state so that the observed decreasing flux could perhaps be related to crystallization of the material. However, if the kinetic predictions are accurate, when the sample was subsequently heated to 400$^{o}$C it should already be fully crystalline, so that a decrease in the pressure versus time curve cannot be ascribed to crystallization of the material. As seen in Figure 5, a decrease in the pressure versus time curve was observed at 400$^{o}$C indicating either i) the kinetic predictions are inaccurate, the material is not fully crystalline when arriving at 400$^{o}$C and subsequent change in dP/dt may still be due to crystallization *or* ii) the decrease in pressure versus time curve is due a property of the measurement system (degassing) and the relatively small changes in the pressure cannot be interpreted as due to structural changes in the sample. Inaccuracies in the kinetic predictions may arise due to the different hydrogen concentration used in the two experiments: 4% $H_2$ for the DSC measurements and 100% $H_2$ used in the permeation measurements possibly leading to different phase transformation pathways and temperatures. In-situ XRD is currently under progress for the examination of case i) and larger samples with increased flux area are under preparation to increase pressure sensitivity range for the examination of case ii). In addition, ex-situ crystallization experiments are underway to examine permeation of metglas materials in the amorphous and crystalline state using room temperature electrochemical permeation setup via ASTM specifications [11].

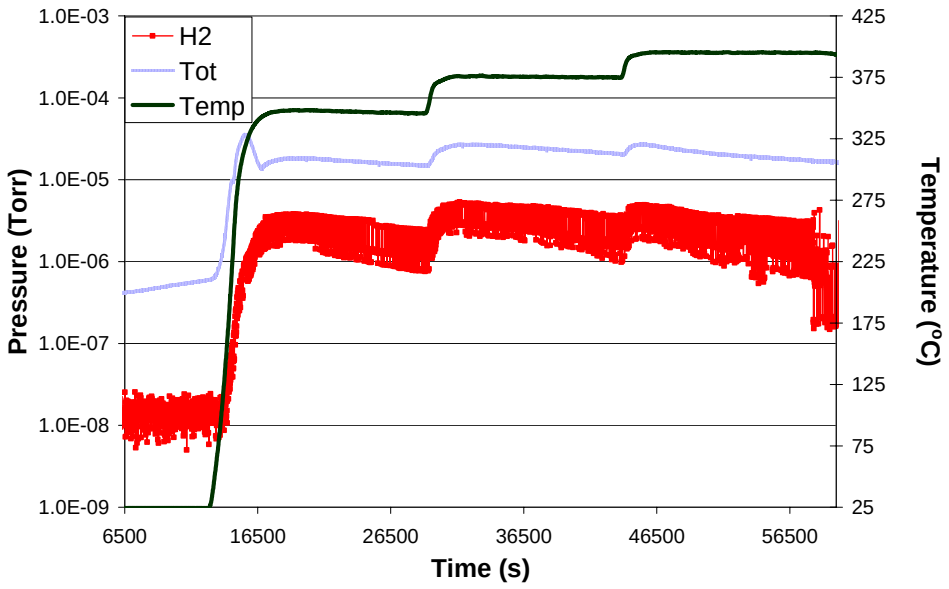


**Figure 5. Pressure in the dynamic hydrogen gas permeation measurement conducted at 350, 380 and 400$^{o}$C as a function of time.**

Presently, the authors are aware of only one recent publication regarding the impact of partial crystallization on the hydrogen permeation properties of amorphous glass in the $Zr_{65}Al_{7.5}Ni_{10}Cu_{12.5}Pd_5$ phase by Yamaura [12]. This material composition forms an icosahedral (i-phase) which precipitates and co-exists within the glass matrix. A near order of magnitude decrease from $10^{-8}$ mol/m s $Pa^{1/2}$ to $10^{-9}$ mol/m s $Pa^{1/2}$ was observed for amorphous and crystalline material respectively at 330°C.

## CONCLUSIONS

The temperature of crystallization, energy released and phase composition/structure identity under argon was determined. Kinetic crystallization parameters based on Avrami equation were obtained for the 2826 alloy and compared with literature. The impact of crystallization on the permeation was studied in-situ by measuring gas phase hydrogen permeation at elevated temperatures. In-situ studies were inconclusive due to the low sensitivity to pressure (hydrogen flux) versus time plots in the dynamic measurement mode and possible system off-gassing during testing. Further experimental work is underway to verify kinetics by structural changes with XRD and to increase the sensitivity of the dynamic permeation measurements in order to sense flux changes due to structural transformations in the material.

## ACKNOWLEDGMENTS

This document was prepared in conjunction with work accomplished under Contract No. DE-AC09-08SR22470 with the U.S. Department of Energy. LDRD funding acknowledged.

## REFERENCES

1. Yamaura, S., et al., *Hydrogen permeation and structural features of melt-spun Ni-Nb-Zr amorphous alloys.* Acta Materialia, 2005. **53**(13): p. 3703-3711.
2. Yamaura, S., et al., *Hydrogen permeation characteristics of melt-spun Ni-Nb-Zr amorphous alloy membranes.* Materials Transactions, 2003. **44**(9): p. 1885-1890.
3. S., S., *Review of Hydroen Isotope Permeability through Materials, Lawrence Livermore National Laboratory Report, UCRL-53441.* 1983.
4. Alfeld G., V.J., *Hydrogen in Metals I., Springer-Verlag, New York.* 1978.
5. Peachey, N.M., R.C. Snow, and R.C. Dye, *Composite Pd/Ta metal membranes for hydrogen separation.* Journal of Membrane Science, 1996. **111**(1): p. 123-133.
6. Patent Pending # 6896750, H.R.C., Howmet Castings an Alcoa Business.
7. Aoki, K., *Amorphous phase formation by hydrogen absorption.* Materials Science and Engineering a-Structural Materials Properties Microstructure and Processing, 2001. **304**: p. 45-53.
8. ASTM E-698-05 Standard Test Method for Arrhenius Kinetic Constants for Thermally Unstable Materials Using Differential Scanning Calorimetry and the Flynn/Wall/Ozawa Method.
9. Morris, D.G., *Crystallization of the Metglas-2826 Amorphous Alloy.* Acta Metallurgica, 1981. **29**(7): p. 1213-1220.
10. Greer, A.L., *Crystallization Kinetics of Fe80b20 Glass.* Acta Metallurgica, 1982. **30**(1): p. 171-192.
11. *ASTM G148-97 Standard Practice for Evaluation of Hydrogen Uptake, Permeation, and Transport in Metals by an Electrochemical Technique.*
12. Yamaura, S.I., et al., *Hydrogen permeation of the Zr65Al7.5Ni10Cu12.5Pd5 alloy in three different microstructures.* Journal of Membrane Science, 2007. **291**(1-2): p. 126-130.